DOI: 10.61782/fa.2025.0277

FORUM ACUSTICUM
EURONOISE 2025

DESIGN OF AN AUTONOMOUS LOW-COST ACOUSTIC ACQUISITION SYSTEM BASED ON INTENSIMETRIC SENSORS FOR UNDERWATER ACOUSTICS SCENARIOS

Pastor Sar, J.D.[1*] **Carbajo San Martín, J.**[2] **Poveda Martínez, P.**[2]
Ramis Soriano, J.[2] **Segovia-Eulogio, E.G.**[3]
[1] IUFACyT, University of Alicante, Spain
[2] Department of Physics, Systems Engineering and Signal Theory, University of Alicante, Spain
[3] Department of Civil Engineering, University of Alicante, Spain

ABSTRACT

The analysis of acoustic signals in a given environment, such as, underwater acoustics, serves as a crucial tool for describing both the physical characteristics of sound and the environmental conditions from a biological standpoint, including biodiversity, species dynamics, and pollution impact. Sound pressure measurements are traditionally performed using microphones or hydrophones connected to acquisition, processing, and storage systems, which are often expensive, bulky, and have limited autonomy. Advances in electronic prototyping technologies have made it possible to develop cost-effective devices capable of acquiring data from a simple sensor or an array of sensors. This study presents the design and development of an autonomous, low-cost acquisition system consists of two pressure sensors yielding an intensity probe to measure sound intensity and particle motion in a single direction. The system allows the configuration of key parameters such as sampling frequency, start and end date/time, and file size, with data stored in a buffer. Tests are performed to assess the system's performance and reliability. The proposed device offers a practical and accessible solution for soundscape monitoring, contributing to environmental analysis and biodiversity studies.

*__Corresponding author__: d.pastor@ua.es.

Keywords: *Soundscape, Autonomous System, Sound Intensity, Particle Motion*

1. INTRODUCTION

The study of soundscapes has gained increasing attention in recent years due to its implications for environmental monitoring, biodiversity conservation, and human well-being. Human activities such as industrial operations, urban expansion, and maritime traffic have increasingly impacted natural soundscapes, raising concerns about acoustic pollution and its effects on ecosystems [1, 2]. Soundscapes defined as the acoustic environments shaped by both natural and anthropogenic sources offer valuable insights into ecological conditions.

One of the main challenges in soundscape research is the ability to capture sound intensity in different media, particularly air and water, with high accuracy and affordability. Traditional hydrophones provide valuable acoustic data in underwater environments, but they often lack the capability to measure absolute sound intensity. This limitation hinders the ability to accurately compare sound levels across different marine habitats and conditions, making it challenging to assess the real impact of anthropogenic noise on underwater ecosystems. Furthermore, the lack of standardized, cost-effective acoustic measurement systems limits large-scale monitoring efforts, making it difficult to assess the long-term impact of noise pollution on ecosystems [3–5].

To address this issue, the use of specialized acoustic measurement systems has been proposed as a viable so-

lution. These systems are designed to measure sound intensity directly, providing more accurate and comparable data than traditional methods. While commercial acoustic sensors are often expensive, recent advances in electronics and microcontroller technology have made it possible to create low-cost alternatives. By leveraging modern, affordable sensors and digital signal processing techniques, these systems allow researchers to collect high-resolution acoustic data efficiently. This approach makes sound analysis more accessible and enables a wider range of applications, from environmental assessments to industrial monitoring [4, 6].

In underwater environments, the application of an intensimetric probe is particularly relevant, as sound propagates in water with different physical properties than in air, the wavelength of incident wave are longer in water because the velocity is higher than in the air. Many underwater species, including fish, rely on acoustic signals for communication and navigation. Increased noise pollution in marine environments has been linked to behavioral changes and disruptions in these communication systems, affecting species' ability to find food, detect predators, and reproduce [7]. Understand these acoustic dynamics is essential for both ecological studies and conservation efforts.

This paper explores the feasibility of developing low-cost acoustic measurement systems, addressing the high cost of current commercial systems. It emphasizes the potential of using affordable electronics and modern sensor technologies to achieve accurate sound intensity measurements. The following sections will discuss the technical aspects of these cost-effective acquisition systems, their applications, and the benefits they offer compared to expensive commercial alternatives.

2. MATERIALS AND METHODS

2.1 Fundamentals of Intensity Meassurements

An intensimetric probe is a specialized instrument designed to measure the intensity of sound in a medium, whether air or water. Unlike conventional microphones or hydrophones that measure sound pressure, intensimetric probes measure both sound pressure and particle velocity, enabling a more accurate assessment of the sound energy within a given space. This allows for the calculation of sound intensity, which represents the amount of sound energy passing through a unit area in a given direction.

Intensimetric probes typically fall into two main categories: pressure-velocity (p-u) probes and pressure-pressure (p-p) probes. A p-u probe consists of a pressure sensor and a dedicated velocity sensor, allowing direct measurement of particle velocity. However, this type of probe is expensive and complex. On the other hand, a p-p probe estimates particle velocity using the pressure gradient between two closely spaced points. While more affordable, p-p probes require careful calibration and signal processing to achieve accurate results.

By capturing both pressure and velocity information, these probes enable sound intensity calculations, making them particularly valuable in environmental monitoring and acoustic studies [3].

The method for measuring sound intensity is based on Newton's second law (mass × acceleration = force), represented by Euler's Relation, eq. 1:

$$\frac{\partial p}{\partial t} = -\nabla p \tag{1}$$

Where p is the pressure, and ∇p is the pressure gradient.

In an arbitrary direction, r, the relationship becomes, eq. 2:

$$\frac{\partial u_r}{\partial t} = -\frac{1}{\rho}\frac{\partial p}{\partial r} \tag{2}$$

Since the pressure gradient is proportional to particle acceleration, the particle velocity can be obtained by integrating the pressure gradient with respect to time, eq. 3:

$$u_r = -\int \frac{1}{\rho}\frac{\partial p}{\partial r} dt \tag{3}$$

In practice, the pressure gradient can be approximated by measuring the pressures at two closely spaced points, A and B, and dividing the pressure difference $P_B - P_A$ by the separation distance Δr. This gives an estimate for the particle velocity component u_r in the direction r, eq. 4:

$$u_r = -\frac{1}{\rho}\int \frac{(P_B - P_A)}{\Delta r} dt \tag{4}$$

This approximation is valid as long as the separation distance Δr is small compared to the wavelength ($\Delta r \ll \lambda$).

Allowing for the measurement of both pressure and the component of the pressure gradient along the line connecting the centers of the microphones. This setup allows for the measurement of the magnitude and direction of the intensity vector component along this line, eq. 5.

$$\hat{I} = -\frac{1}{2\rho\Delta r}\overline{(P_A + P_B)\int (P_B - P_A)dt} \qquad (5)$$

It is important to note that it is the phase gradient of the pressure that results in a non-zero real intensity vector.

Making the FFT (Fast Fourier Transform) of both signal (Left and Right channels), eq. 6, an analyzer can be employed for intensity calculations within the FFT limitations (blockwise analysis). The intensity can be derived from the imaginary part of the cross-spectrum between the two microphone signals. The relationship is expressed as:

$$\hat{I} = -\frac{1}{w\rho\Delta r} Im(G_{AB}) \qquad (6)$$

This method is commonly used for calculating sound intensity today.

2.2 Hardware and Software Components

In this study, different components were used to develop the data acquisition and processing system. The main element of the system is the ESP32-WROOM-32D, a versatile microcontroller equipped with Wi-Fi and Bluetooth capabilities. This microcontroller handles the primary control tasks, including data collection, processing, and communication. To ensure data conversion, an ADC I2S was employed, enabling the conversion of analog signals from the piezoelectric sensor into digital data using the I2S protocol. This ADC was critical for the sensor's behaviour. It supports both 16-bit and 24-bit resolution; however, since it operates in slave mode with the ESP as the master, it is limited to 16-bit operation.

A Real-Time Clock (RTC) module was integrated into the system to maintain the current time and date. Its primary function is to allow the user to select the start and end time for data collection, ensuring accurate and synchronized operation. Additionally, the RTC enables the system to generate filenames that include the current date, making it easier to organize and identify recorded files chronologically. To store the collected data, an SD Card Writer Module was utilized, providing a reliable and accessible method for saving large amounts of sensor data for further analysis.

The system was powered using a battery module, which allows for autonomous operation of the ESP32 microcontroller over extended periods without needing a direct supply connection. To ensure proper signal transfer between the piezoelectric sensor (PIC255) and the ADC, a buffer to work as impedance matcher was used. This adapter adjusted the impedance of the piezo sensor to that of the ADC, helping to preserve the amplitude of the signal.

The entire system, including the sensor and other critical components, see Fig.1, was housed in a custom-designed 3D-printed structure, providing a secure mounting solution. Finally, the components were encapsulated using a low-viscosity unfilled epoxy resin with a reactive diluent (PX771C). This material was selected to conform to the sensor's geometry, preventing water ingress while having minimal impact on the sensor's performance. In addition to providing environmental protection, the use of resin also served to improve impedance matching between the sensor and its surrounding medium, enhancing the efficiency of signal transmission.

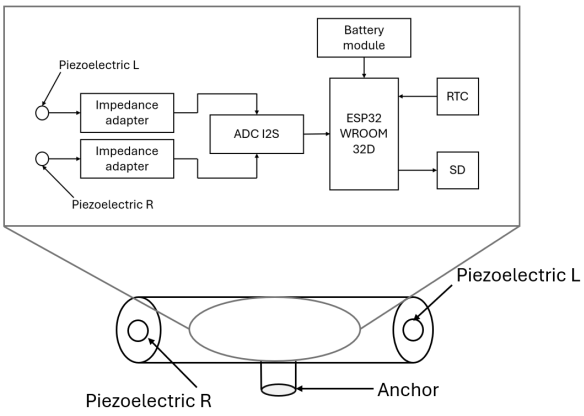

Figure 1. Acquisition system and internal connections

To effectively manage the operation of the system, dedicated software was developed to control the recording process and ensure reliable data acquisition. This software is crucial for coordinating the various hardware components while optimizing performance and energy efficiency. It leverages the AudioTools.h library, developed by Phil Schatzmann, to manage I2S audio streaming, allowing real-time conversion of analog signals from the sensor into digital format. Bluetooth communication is integrated for remote configuration, enabling users to adjust key sampling parameters such as bit depth, number of channels, and recording duration. A Real-Time Clock (RTC) module is used to synchronize scheduled recordings, ensuring data is collected at the intended times. Captured data is stored on an SD card for later analysis. To

maximize energy efficiency, the ESP32 microcontroller enters deep-sleep mode between recordings, see Fig. 2, significantly extending the system's operational lifespan making it suitable for long-term monitoring applications.

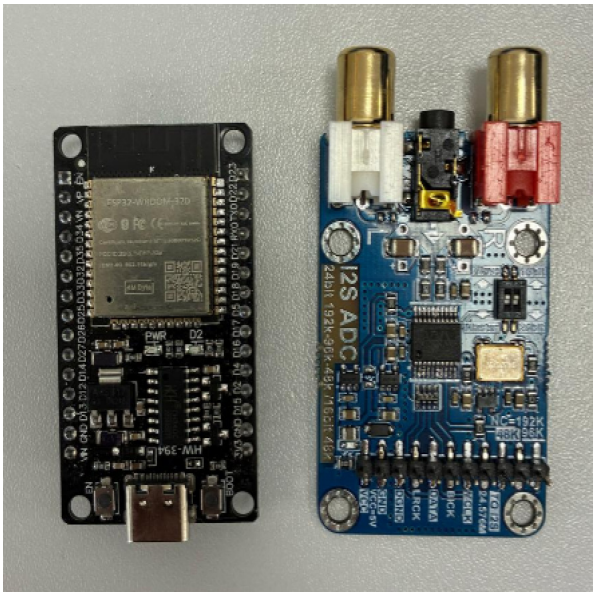

Figure 2. Main elements of the adquisition system, ESP32 and ADC I2S

2.3 Geometrical Configurations and Experimental Considerations

The measurement system is designed to be housed within different geometrical enclosures, see Fig. 3, each offering unique advantages depending on the experimental setup. Three possible configurations were studied: a spherical enclosure, a cylindrical enclosure, and an arrowhead-like geometry. The first consists of a sphere with a 15 cm diameter, providing a design that minimizes directional biases and allows for uniform pressure distribution around the sensors. The second is designed offering a compact structure with a controlled sensing axis and the arrowhead-like geometry features a 15 cm long structure with a 10 cm radius, enhances directional sensitivity by aligning with pressure gradients. Its streamlined design is optimized, making it ideal for cases where significant variations in directionality occur.

A numerical study was conducted to study the interaction between the acoustic field with the three structures studied, see Figure 3, this study was maked with FEM (Finite Element Method), simulating an acoustic field within a 0.3 m domain. The plane waves, set a variation between 0º and 180º incidence angle relative to the sensor's normal, replicate real-world acoustic conditions. The enclosures were modeled with epoxy resin and the structure like rigid walss, including a density of 1100 kg/m³, a Young's modulus of 3.3 GPa, and a Poisson's ratio of 0.35, among others.

To ensure accurate results, a tetrahedral mesh was applied, with size constraints based on frequency dependent parameters, making the mesh for the smaller elements in therms of $\lambda/6$.

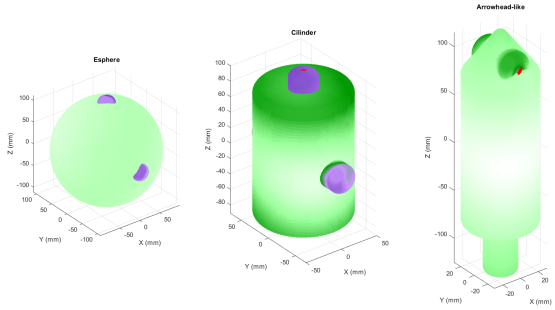

Figure 3. Geometries studied, red doths (symmetrical piezoelectric possitions in the geometry)

The system integrates two piezoelectric transducers strategically positioned to enable pressure gradient measurements. The system has been tested with several transducer configurations to evaluate their effectiveness in acoustic and pressure measurements. One studied configuration involves a spherical enclosure, where two piezoelectric sensors are positioned on opposite poles one at the top and the other at the bottom aligned along the vertical (Z) axis. This symmetrical setup is intended to capture pressure variations propagating longitudinally through the center of the sphere.

Another tested design is a cylindrical enclosure with a similar axial alignment, where the two transducers are also mounted at the top and bottom ends. This configuration maintains a comparable geometry to the sphere but allows for alternative mechanical integration and directional response due to its elongated shape.

A third configuration explored is the arrowhead-shaped enclosure, which houses both sensors near the pointed end. This design focuses on capturing pressure changes originating from the front or tip of the structure, making it particularly suitable for directional measurements in environments where pressure waves are expected

to approach from a specific direction.

Also several tests were conducted to evaluate the performance and reliability of the system under various configurations and operational conditions. These tests focused on key parameters, including sampling frequency (fs), bit depth per sample, recording duration, buffer configuration (number of buffers and samples per buffer), signal to noise ratio (SNR), and total harmonic distortion (THD) for all the possibles configurations of the electronic system. A sampling frequency tests aimed to determine the optimal fs value for capturing acoustic signals while balancing resolution and data storage efficiency. Higher sampling rates improve sound quality but require more memory, while lower rates save storage space but may lose finer details in high frequencies. The system was tested at 44.1 kHz, 48 kHz, and 96 kHz. The bit depth per sample tests were conducted to analyze the impact of quantization levels on signal accuracy. The system was tested with 16-bit and 32-bit storage formats, buffer configuration tests examined the impact of buffer size and count on real-time performance. Various setups were tested to optimize data acquisition, minimize delays, and ensure smooth operation. The final configuration balanced response time and memory efficiency, preventing data loss.

To externally evaluate the system's performance, two hydrophones were connected along an arbitrary spatial direction (r), separated by a distance of $\Delta r = 6\,\text{cm}$. These hydrophones were linked to a phantom generator, which was in turn connected to a B&K Nexus signal conditioner. Subsequently, a stereo signal was fed into the sensor electronics to compute the acoustic intensity. The system was tested at frequencies of 1 kHz and 250 Hz. Measurements were conducted in two configurations: one with the radiation pattern aligned along the normal direction of the source (DML) and another with the pattern perpendicular to the source. These experimental setups aim to assess how the system behaves under external testing conditions.

3. RESULTS AND DISCUSSIONS

3.1 Performance Evaluation and Signal Integrity Analysis

Since the system processes data in 32-bit words, using 16-bit or 24-bit formats reduces precision but does not introduce significant quantization artifacts or aliasing. To mitigate this, a low-pass filtering process must be applied before reducing the bit depth, ensuring that unwanted high-frequency components do not affect the integrity of the recorded signals. The tests confirmed that filtering before downsampling is essential for maintaining signal fidelity, see Fig. 4.

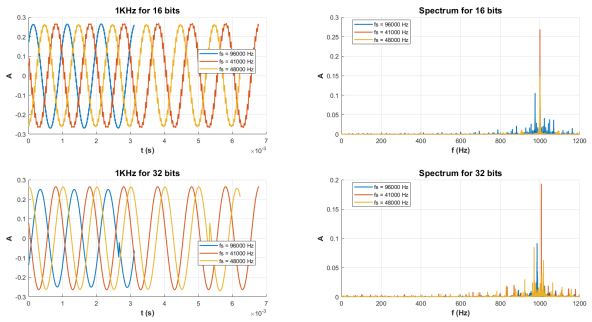

Figure 4. Signal of 1KHz captured at diferent fs and different bith dephts

Recording duration tests evaluated the system's ability to acquire signals continuously despite the ESP32's limited RAM (200–300 KB). Buffer optimization was key to preventing data loss. Optimal configurations included 16 buffers of 2048 samples for 44.1 kHz and 48 kHz, and 8 buffers of 1024 samples for 96 kHz, ensuring smooth data acquisition and preventing memory overflows.

SNR and THD evaluations assessed signal integrity using a 1 kHz, 200 mVpp sine wave. SNR was measured within a ±10 Hz window around the fundamental frequency, while THD was calculated from the first seven harmonics. Results showed that lower bit depths increased noise, whereas higher bit depths improved signal fidelity, see Tab. 1.

Table 1. SNR and THD values at different sample rates and bit depths

fs / bits	44.1 kHz	48 kHz	96 kHz
SNR (dB) (16-bit)	18.86	12.61	0.05
SNR (dB) (32-bit)	12.05	-3.20	4.57
THD (dB) (16-bit)	-61.67	-59.46	-46.83
THD (dB) (32-bit)	-54.50	-51.04	-48.28

Saturation was observed in the system when the input signal exceeded a 1 Vpp (Volt peak-to-peak) threshold. Beyond this level, the system could no longer capture the signal's details accurately, resulting in clipping and signal

distortion. This effect can be seen in Fig. 5 for the 16-bit captures at fs = 44.1 kHz. The Total Harmonic Distortion (THD) was also analyzed for different input signal amplitudes, as shown in Tab. 2.

Table 2. THD for each amplitude

Amplitude (mVpp)	200	400	600	800	1000
THD (dB)	-61.67	-61.72	-57.19	-41.38	-20.36

The results indicate that THD remains relatively low and stable for amplitudes up to 600 mVpp. However, as the input signal increases beyond this point, THD rises significantly, reaching -20.36 dB at 1 Vpp. This suggests that the system approaches its saturation limit at higher amplitudes, leading to increased distortion, potential signal clipping, and reduced measurement accuracy.

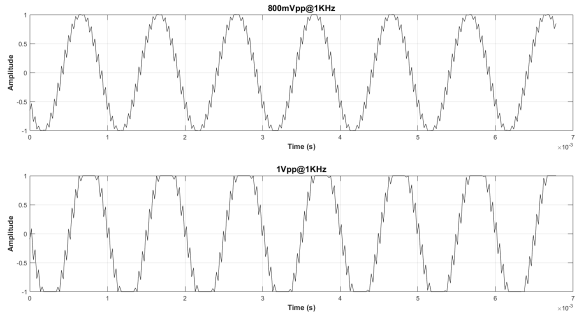

Figure 5. Signal captured at fs = 44100Hz with 16 bits at 800mVpp and 1Vpp

3.2 Numerical Study of Configurations and Materials

The pressure field, intensity field and angles in water for the different sensor geometries were analyzed at frequencies of 100, 1000, and 5000 Hz, see Fig. 6. Among the three geometries, the spherical design exhibited the most consistent and focused pressure distribution. This configuration minimizes energy loss and enhances the efficiency of sound wave propagation, providing a clearer and more accurate acoustic signal compared to the cylinder and arrowhead geometries.

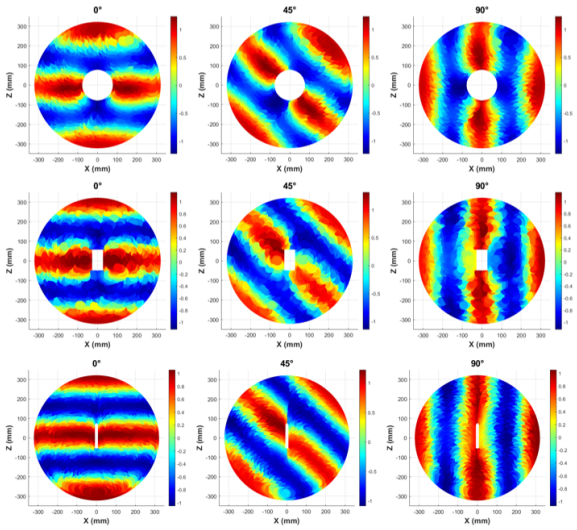

Figure 6. Pressure field and intensity field in water with the different geometries studied for 5000 Hz

The acoustical intensity calculated through the pressure gradient method showed values of 1.1623×10^{-6} for 100 Hz, 2.3410×10^{-6} for 1000 Hz, and 2.4877×10^{-6} for 5000 Hz at 0º without any geometry. The spherical geometry consistently outperformed the other configurations in energy concentration, showing better sensitivity and alignment with wave propagation, see Tab. 3. This can be attributed to its symmetrical shape and axial sensor placement, which enhance the detection of longitudinal pressure variations. In contrast, the cylindrical and arrowhead geometries exhibited lower intensity due to reduced directivity and possible misalignment with the wavefront.

Table 3. Acoustic intensity (W/m^2) for each geometry and angle

Frequency (Hz)	100	1000	5000
Sphere 0º	1.2781×10^{-6}	2.5162×10^{-6}	2.6929×10^{-6}
Sphere 45º	5.7292×10^{-7}	1.1210×10^{-6}	1.3863×10^{-6}
Sphere 90º	1.2409×10^{-12}	2.8342×10^{-12}	5.5164×10^{-12}
Cylinder 0º	4.9366×10^{-7}	9.4865×10^{-7}	1.0685×10^{-6}
Cylinder 45º	2.1438×10^{-7}	3.9884×10^{-7}	4.2466×10^{-7}
Cylinder 90º	2.3352×10^{-11}	3.2960×10^{-10}	1.9763×10^{-9}
Arrowhead 0º	3.7027×10^{-12}	8.4484×10^{-12}	1.0831×10^{-11}
Arrowhead 45º	1.4429×10^{-12}	3.4910×10^{-12}	6.3566×10^{-12}
Arrowhead 90º	1.4312×10^{-13}	3.5058×10^{-13}	1.8272×10^{-12}

3.3 Preliminary Experimental Evaluation

Fig. 8 shows the recorded signals obtained at 1 kHz for both experimental configurations: with the radiation pattern aligned along the normal direction of the source (DML) and with it oriented perpendicularly. In both cases, the signals captured by the two hydrophones exhibit the expected sinusoidal behavior and maintain a stable phase relationship over time. The observable phase shift between the channels confirms that the wave propagation direction is appropriately captured, allowing for a valid estimation of the acoustic intensity.

The corresponding frequency spectrum confirms a dominant peak at 1 kHz, with minimal spectral leakage or noise, indicating a clean and well-defined excitation. Using the temporal signals, the cross-spectrum was computed, and the imaginary component was used to estimate the acoustic intensity via the established method. The results confirm that the system is capable of resolving the intensity vector under controlled excitation conditions, validating the effectiveness of the signal processing approach.

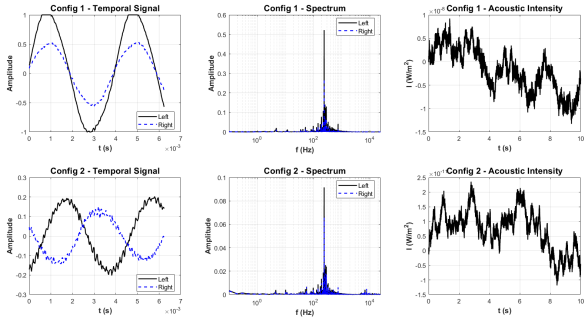

Figure 7. Temporal signal captured by the system, spectrum and calculated intensity for 1KHz pure tone

Additionally, the Total Harmonic Distortion (THD) and Signal-to-Noise Ratio (SNR) were analyzed for all experimental cases, as shown in Tab. 4. The THD values were found to be minimal across all configurations, indicating that the system produces signals with a low level of harmonic distortion, ensuring accurate representation of the primary acoustic signal. Furthermore, the SNR was consistently high, confirming that the system is able to effectively distinguish the desired signal from background noise. These results demonstrate a favorable signal quality across all tested configurations, supporting the system's reliability for precise acoustic intensity measurements.

Table 4. SNR and THD values for Left and Right channels in different experimental cases

Cases	SNR (dB) L	SNR (dB) R	THD (dB) L	THD (dB) R
250Hz Conf.1	43.24	37.97	-37.47	-47.45
250Hz Conf.2	29.35	-48.00	-32.47	-43.67
1KHz Conf.1	34.33	27.67	-37.23	-43.11
1KHz Conf.2	28.65	35.56	-28.07	-40.02

4. CONCLUSIONS

The measurement system developed in this study offers high adaptability through three geometric configurations spherical, cylindrical, and arrowhead like each tailored for different experimental needs. The spherical design provides uniform pressure distribution, the cylindrical allows for directional control, and the arrowhead enhances sensitivity. This flexibility makes the system suitable for a wide range of acoustic research applications requiring varied orientations and pressure resolutions.

The performance tests of the system, which included analysis of sampling frequency, bit depth, recording duration, and buffer configurations, demonstrated the system's ability to handle acoustic signals with high fidelity, adjusting its parameters to prevent data loss or distortion. Optimal buffer and sampling frequency configurations (44.1 kHz and 48 kHz) were identified to balance real-time performance and memory efficiency, while the 96 kHz configuration proved suitable only for specific cases. The tests also confirmed the importance of proper anti-aliasing filtering and avoiding system saturation, ensuring accurate signal capture.

Finally, both numerical and experimental studies highlighted the impact of the enclosure geometry and transducer positioning on the system's acoustic and structural performance. The results emphasized the need to carefully select the configuration and parameters based on the specific experimental setup to achieve the best accuracy and reliability in measurements. Moreover, the system's flexible design and low power consumption suggest the potential for developing low-cost sensors with sufficient autonomy to perform long-duration measurements, opening up possibilities for applications in continuous or remote monitoring scenarios.

5. ACKNOWLEDGMENTS

This publication is part of the project PID2021-127426OB-C22, funded by MCIN/AEI/10.13039/501100011033 and by the European Union "NextGenerationEU"/PRTR. The reference

mentioned corresponds to the grant resolution. MCIN stands for the Ministry of Science and Innovation; AEI is the acronym for the State Research Agency; 10.13039/501100011033 is the Digital Object Identifier (DOI) of the Agency; and PRTR stands for the Recovery, Transformation and Resilience Plan. This work is also part of the research project PID2021-127426OB-C22, funded by the Ministry of Science and Innovation, the State Research Agency (MCIN/AEI /10.13039/501100011033), and the European Regional Development Fund (FEDER, EU)

6. REFERENCES

[1] A. Farina, *Soundscape Ecology: Principles, Patterns, Methods and Applications*. Dordrecht, Netherlands: Springer, 2014.

[2] B. C. Pijanowski, L. J. Villanueva-Rivera, S. L. Dumyahn, A. Farina, B. L. Krause, B. M. Napoletano, N. Pieretti, and J. C. Alvarado, "Soundscape ecology: The science of sound in the landscape," *BioScience*, vol. 61, no. 3, pp. 203–216, 2011.

[3] B. . Kjaer, "The fundamentals of sound intensity measurement," in *Technical Review No. 3*, (Nærum, Denmark), pp. 3–43, 1982.

[4] R. Hickling, *Sound-Power Flow: A Practitioner's Handbook for Sound Intensity*. San Rafael, CA: Morgan & Claypool Publishers, 2016.

[5] J. D. Pastor Sar, J. Carbajo San Martín, P. Poveda Martinez, J. Ramis Soriano, and E. G. Segovia-Eulogio, "Preliminary design of a particle motion sensor for underwater applications," in *Proceedings of Acústica 2024*, (Faro, Portugal), pp. 490–499, 2024.

[6] E. M. Fischell, K. Railey, O. A. Viquez, and H. Schmidt, "Passive tracking of autonomous underwater vehicles (auvs) using a low-cost acoustic data collection system," *The Journal of the Acoustical Society of America*, vol. 141, no. 5, p. 3916, 2017.

[7] A. N. Popper and A. D. Hawkins, "An overview of fish bioacoustics and the impacts of anthropogenic sounds on fishes," *Journal of Fish Biology*, vol. 94, no. 2, pp. 315–329, 2019.